Volume 3, Number 1: 23-29, October 2005
Review Article

International Journal of
Vascular Biomedical Engineering

Computational study of the wave propagation in three-dimensional human cardiac tissue

Soon Sung Kwon[1], Uk Bin Im[1], Ki Woong Kim[2], Yong Ho Lee[2] and Eun Bo Shim[1¶]

[1]*Department of Mechanical & Biomedical Engineering, Kangwon National University*

[2]*Bio-signal Research Laboratory, Korea Research Institute of Standards and Science,*

Abstract

We developed a three dimensional cardiac tissue model based on human cardiac cell and mono-domain approximation for action potential propagation. The human myocyte model proposed by ten Tusscher *et al.* (TNNP model) (2004) for cell electrophysiology and a mono-domain method for electric wave propagation are used to simulate the cardiac tissue propagation mechanism using a finite element method. To delineate non-homogeneity across cardiac tissue layer, we used three types of cardiac cell models. Ansiotropic effect of action potential propagation is also considered in this study. In this 3D anisotropic cardiac tissue with three cell layers, we generated a reentrant wave using S1-S2 protocol. Computational results showed that the reentrant wave was affected by the anisotropic properties of the cells. To test the reentrant wave under pathological state, we simulated a hypertopic model with non-excitable fibroblasts in stochastic manner. Compared with normal tissue, the hypertropic tissue result showed another center of reentrant wave, indicating that the wave pattern can be more easily changed from regular with a concentric focus to irregular multi-focused reentrant waves in case of patients with hypertrophy.

Key words: Reentrant wave in a cardiac tissue, Mono-domain method, Hypertropic tissue model

Introduction

Arrhythmia is one of the major causes of human cardiac death. It is well known that a reentrant wave in cardiac tissue can be a source of tachycardia and Torsade de Pointes. Stationary or drifting reentry wave patterns in cardiac tissue are closely related to tissue physiological properties. Especially the wave patterns in diseased tissue are critical for the generation of arrhythmic chaos resulting in the sudden cardiac death of heart failure patients. Progressive development of heart failure is accompanied by hypertrophy, a ventricular wall thickening. According to the progress of hypertrophy, a large portion of cardiac tissue is occupied by electrically non-excitable fibroblasts. Therefore, elaborated study on the reentrant wave dynamics in the condition of cardiac hypertrophy is needed to elucidate the mechanism of sudden cardiac death due to arrhythmias.

Along with experimental works, a lot of computational works have been done to delineate the mechanism of reentrant wave with its underlying cellular phenomena (Xie et al. 2004, Rudy 2000, Gima and Rudy 2002). Fenton et al. (2002) has provided multiple mechanisms of reentrant wave break-up. In real ventricular geometry, Berefeld and Jalife (1998) investigated the interaction of ventricular tissue with Purkinje fibers in reentrant wave dynamics. As a diseased cardiac tissue model, Usyk and McCulloch (2003) presented the electromechanical

¶ 200-701, hyoja-dong, chuncheon, kangwon, Korea
E-mail: ebshim@kangwon.ac.kr

model of cardiac resynchronization in the dilated heart. Though there have been a lot of computational studies have been made for delineation of reentrant wave dynamics in cardiac tissue, the effect of fibroblasts in hypertrophy has not been well described. Non-excitable fibroblasts increased as progress of hypertrophy. As demonstrated in the experiment by Gaudesius et al. (2003), the non-excitable media such as fibroblasts can induce a significant delay of electric wave propagation eventually resulting in arrhythmias. Therefore, we investigate the effect of non-excitable fibroblasts on the reentrant wave dynamics in hypertropic tissue to delineate the mechanism of sudden cardiac death due to arrhythmias in heart disease patients.

Though the cardiac cell models based animal cardiomyocyte have been presented by several research groups (Luo and Rudy 1993, Noble et al. 1998, Matsuoka et al. 2004), the model for human ventricular cell model was not popular. Priebe and Beuckelmann (PB model) (1998) has proposed a human ventricular cell model and simulated pathological state of the cellular phenomena using the model. Recently, Ten Tusscher *et al.* (TNNP model, 2004) proposed an improved human myocyte cell model incorporating the recent experimental data on the major ionic currents: the fast Na^+, L-type Ca^{2+}, transient outward, rapid, and slow-delayed rectifier K^+ currents. In this study, we presented computational results of reentrant wave dynamics in a hypertropic tissue using a three dimensional model of human cardiac tissue. The mono-domain modeling implemented by a finite element method is used to simulate the cardiac tissue propagation. Three kinds of cardiac cell models are used to model inhomogeneous cell types across ventricular wall layer. Ansiotropic effect of action potential propagation according to cardiac fiber orientation is also implemented using a directional diffusivity tensor. To simulate the hypertropic effect on reentrant wave dynamics, we randomly distributed no-excitable cells in the computational domains.

Material and Method

Governing equation for electric wave propagation of cardiac tissue

The TNNP model of a human ventricular cell is used. This includes recent experimental data on most of the major ionic currents: the fast Na^+, L-type Ca^{2+}, transient outward, rapid, and slow-delayed rectifier K^+ currents (Appendix A). We used the model without any change from the original formulation. This is inserted into the tissue model using a mono-domain approximation (or simplified bidomain method) of cardiac tissue. In the bidomain method, cardiac tissue is divided into two interpenetrating domains, intracellular (IC) and extracellular (EC), separated by an excitable membrane. Considering that ion current flux coming out from IC should enter all to EC part, we can derive the following conservation equation as follows:

$$\frac{\partial V_m}{\partial t} = -\left(I_{ion} + I_{app}\right)\frac{1}{C_m} + \left(\nabla \cdot D_i \nabla V_m - \nabla \cdot D_i \nabla \phi_e\right)\frac{1}{C_m \beta} \quad (1)$$

In Eq. (1), V_m is a transmembrane voltage defined as $V_m = (\phi_i - \phi_e)$ where ϕ_i and ϕ_e denote IC and EC potentials, respectively. D_i and D_e represent the electric conductivity tensors in IC and EC. I_{app} is a stimulus current and I_{ion} denotes the sum of the ion currents through cell membrane. β and C_m are the surface to volume ratio and cell capacitance per unit surface area, respectively. In the mono-domain method, ϕ_e is assumed to be constant and the resulting equation is obtained.

$$\frac{\partial V_m}{\partial t} = -\frac{\left(I_{ion} + I_{app}\right)}{C_m} + \frac{1}{C_m \beta}\nabla \cdot D_i \nabla V_m \quad (2)$$

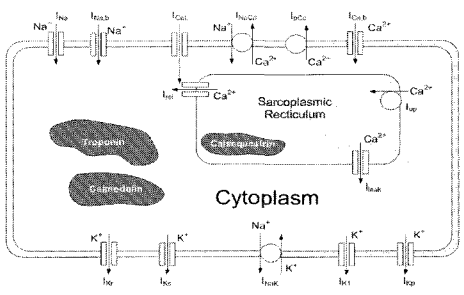

Figure 1. Schematic of the human ventricular cell model proposed by Ten Tusscher et al.

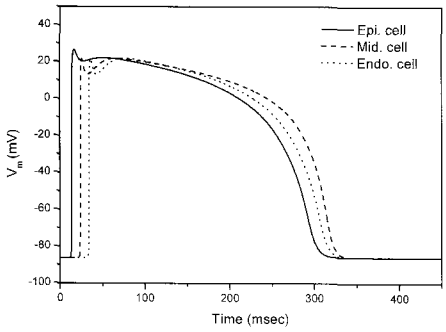

Figure 2. Action potential transients for three cell types in TNNP model.

Finite element formulation of the monodomain equation

In Eq. (2), the time derivative is discretized using an Euler method whereas a Galerkin method is applied to the partial derivative for the diffusion term as follows:

$$\int_\Omega W\frac{V_m^{n+1}-V_m^n}{\Delta t}d\Omega = -\int_\Omega W\left(\frac{I_{ion}+I_{stim}}{C_m}\right)d\Omega - \int_\Omega\left(D_i\nabla W\cdot\nabla V_m^n\right)d\Omega \quad (3)$$

Here, W means a weighting function and superscript 'n' represents a time index during time marching. Then we approximate the variable V_m within the computational domain by the interpolation function that is equal to the weight function W in Galerkin method at each nodal point of computational mesh as follows:

$$V_m^{\%} = \sum_i W_i\left(V_m\right)_i \quad \text{(i: grid node point index)} \quad (4)$$

When we insert Eq (4) into (3) and summarize the equation, we can get the resulting algebraic equation represented by matrix problem using tensor notation.

$$M_{ij}\left(V_m\right)_j^{(n+1)} = M_{ij}\left(V_m\right)_j^{(n)} + S_i^{(n)} - K_{ij}\left(V_m\right)_j^{(n)} \quad (5)$$

$$M_{ij} = \int_\Omega\left(\frac{W_i W_j}{\Delta t}\right)d\Omega \quad (6)$$

$$K_{ij} = \int_\Omega\left(D\nabla W_i\cdot\nabla W_j\right)d\Omega \quad (7)$$

$$S_i^{(n)} = -\int_\Omega W_i\left(\frac{I_{ion}+I_{stim}}{C_m}\right)d\Omega \quad (8)$$

Here, M_{ij}, K_{ij}, and S_i represent mass, diffusion and reaction matrices, respectively. If we simplify M_{ij} as lumped mass M_{ii} to avoid matrix inversion in Eq. (5), we can get the following equation.

$$\left(V_m\right)_i^{(n+1)} = \left(V_m\right)_i^{(n)} + S_i^{(n)} - U_i^{(n)} + V_i^{(n)}$$
$$\left(U_i^{(n)} = K_{ij}\left(V_m\right)_j^{(n)}/M_{ii},\quad V_i^{(n)} = K_{ij}\left(\phi_e\right)_j^{(n)}/M_{ii}\right) \quad (9)$$

Eq. (9) is solved using the operator splitting scheme proposed by Qu and Garfinkel (1999). During the computation of the reaction matrix S_i, it is needed to compute the cell electrophysiological properties at every node point of the computational mesh. In the operator splitting scheme, the time variations of cell properties such as membrane voltage, ion concentrations, membrane channel activity are computed at the computational nodes (reaction step) and these cell-level membrane potential are diffused into the ventricular tissue (diffusion step). More details on the operator splitting scheme and mono-domain method are represented in the references (Qu and Garfinkel 1999).

Pseudo ECG signal computation

Pseudo ECG is calculated for the present 3D tissue model by summing up all the trans-membrane intercellular dipoles (P) weighted by the distance (r) from the electrode and its direction (Berenfeld and Jalife, 1998).

$$ECG(t) = -\sum_{nodes}\frac{\vec{P}(t)\cdot\vec{r}}{r^3} \quad (10)$$

The dipole was proportional to the trans-membrane potential gradient, and we assumed the electrode was at the location away from epicardial surface from 3 cm (Gima and Luo, 2002).

Results

Cellular model

First we presented the cellular results using the TNNP model. The schematic of the TNNP model is depicted in Fig. 1, representing ion channels, ion pump across cell membrane and intracellular calcium dynamics. The shape of the action potential and the Ca^{2+} transient from the TNNP model were well reconstructed for the 1.0 sec cardiac cycle (Fig. 2). The action potential shows the characteristic spike notch dome shape found for human cardiac cells with a resting potential of −87.3 mV. The maximum plateau potential is +21.7 mV, and the durations of the action potential at 90% repolarization are approximately 265, 325, and 280 msec for epicardial, midcardial, and endocardial cells, respectively.

Tissue 3D baseline model

The schematic of the 3D is shown in Fig. 3. Width is 12 cm x 12 cm and depth in z-axis is 1.5 cm. The number of the total mesh in x, y, z direction is 90, 90, and 20, respectively. We used a S1-S2 protocol described in Fenton et al. (2002) to induce a spiral wave in tissue plane. Initially the cells located in the boundary surface of x=9 cm are stimulated and the depolarization wave travels along the decreasing x direction (S1 protocol). When repolarization wave passes through the plane of x=4.5 cm, the half of the depolarized domain is reset to the initial condition to induce instability (S2 protocol). In the present simulation, S2 protocol was imposed at t = 400 msec. We computed here three cases as baseline simulations: isotropic simulation only with epicardial cell layer, anisotropic one only with epicardial cell layer, and anisotropic one with three layers, epicardial, midcardial, and endocardial cell layers. Each cell layer has an equal thickness through z direction. In case of anisotropic simulation, the conduction diffusivity tensor, D_i, has different values according to fiber orientation. Here the fiber orientations through tissue layer vary linearly from -60° (endocardium) to +60° (epicardium) as suggested by Beyar and Landersberg (1984). We also assume that the conduction coefficient in fiber

Table 1 Simulation conditions for the action potential propagation through ventricular tissue.

Simulation conditions	Values	References
Diffusion coefficient Along fiber orientation Normal to fiber orientation	$D_{\parallel}$=0.00154 cm^2/msec $D_{\perp}$=1/7*$D_{\parallel}$=0.00022 cm^2/msec	Ten Tusscher et al. (2005) Clayton & Holden (2002)
Cell capacitance per unit surface area	C_m=2 μF/cm^2	Ten Tusscher et al. (2005)
Time step size	0.01 msec	Model parameter
Initial values of the model variables Action potential baseline value Intracellular Ca^{2+} concentration	-87.3 mV 0.2 μM	Ten Tusscher et al. (2005) Ten Tusscher et al. (2005)
Stimulus conditions Stimulus magnitude Stimulus duration	50 pA/pF 1 msec	Model parameter Model parameter

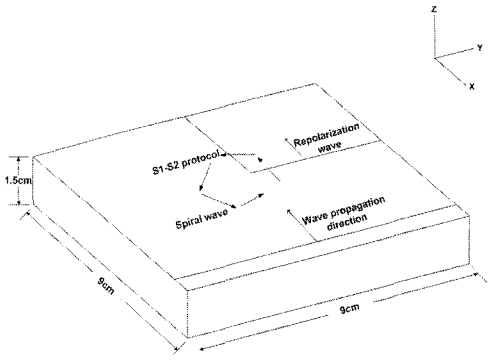

Figure 3. Schematic of a three dimensional tissue model with the description of wave propagation and S1-S2 protocol for inducing spiral wave.

orientation is 7 times larger than that in the normal direction of fiber orientation (Clayton and Holden, 2002). Detailed simulation conditions are summarized in Table 1.

Fig. 4 shows the sequential plots of action potential contour before the reentrant wave is fully developed. Depolarization wave is shown in Fig. 4(a), traveling in negative x direction. Repolarization wave passing through the mid plane is plotted in Fig. 4(b) before the S2 protocol is applied. Due to sharp corner formed by the S1-S2 protocol near the center of the computational domain, instability of action potential traveling wave happens and thus the spiral wave begin to generate as shown in Fig. 4(c) and (d). In Fig. 5, we presented the action potential contours of the fully developed spiral wave for different simulation conditions. For isotropic case, the spiral wave didn't have any variation across thickness or fiber orientation (Fig. 5(a)) whereas anisotropic one showed different pattern of spiral wave. Deformed spiral wave structure was found for anisotropic cases, biased to the fiber orientation. The wave for anisotropic case with only an epicardial cell layer was biased in the fiber orientation but no variation across tissue thickness (Fig. 5(b)) whereas an action potential gradient across tissue thickness was observed (Fig. 5(c)). When we compared the equipotential surfaces (AP = 0 mV) of the three cases, the anisotropic case with three cell layers showed a twisted pattern along fiber direction and thickness layer, indicating the augmentation of wave complexity by the cellular inhomogenity and anisotropic conduction. Pseudo ECG

changes were plotted in Fig. 6. ECG pattern of the isotropic case was regular and had a high frequency with duration of 287 msec in Fig. 6(a) whereas oscillatory pattern with varying magnitude was observed and frequency was relatively low for that of the anisotropic case with three cell layers (Fig. 6(b)).

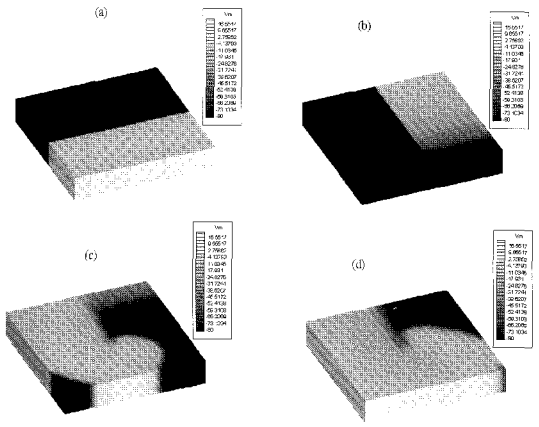

Figure 4. Sequential contours of action potential for isotropic tissue model. (a) t=200 msec, (b) t=400 msec, (c) t=600 msec, (d) t=800 msec.

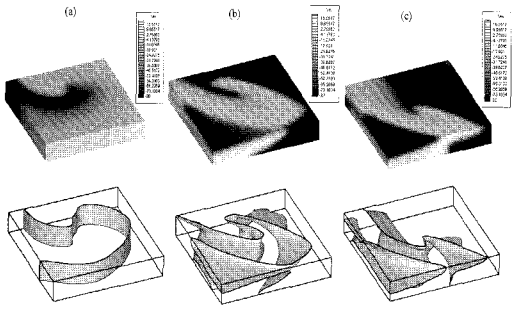

Figure 5. Action potential patterns for three different models. (a) Isotropic model, (b) Anisotropic model with epicardial cell layer, (c) Anisotropic model with three cell layers.

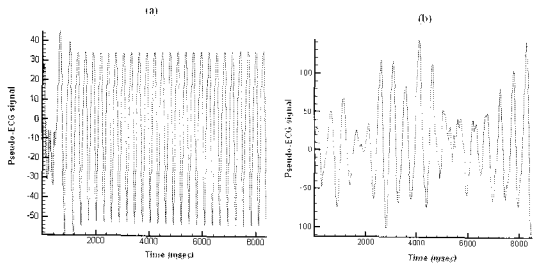

Figure 6. Pseudo ECG patterns. (a) Isotropic model, (b) Anisotropic model with three cell layers.

3D hypertropic tissue model

Cardiomyopathy is the pathological states where the muscle layer become thick and the portion of non-excitable fibroblasts is gradually increases as the progress of disease, eventually resulting in heart failure. Due to increased percentage of non-excitable fibroblasts, the propagation of electric wave is hindered. To simulate the effect of this diseased state of tissue on spiral wave propagation, we constructed an hypertropic model of ventricular tissue.

To incorporate the role of non-excitable fibroblasts into the model, we first determined a conductivity of fibroblasts mixed with cardiac cells from a recent experimental observation done by Gaudesius *et al.* (2003). They measured the electric propagation time in a line of ventricular cells partially mixed with fibroblasts and found that the fibroblasts of 15% length in the entire cell line can delay wave propagation by 30 msec. A simple one-dimensional simulation prior to a three dimensional computation was done to specify the conductivity of fibroblasts. Fig. 7 shows the activation delay time of electric excitation due to the fibroblasts in the cell line in the similar protocol with the experiment (Gaudesius *et al.*, 2003). According to the decrease of the electric conductivity values of fibroblasts as shown in Fig. 7, the activation delay time was increased. In case of the fibroblasts conductivity value of $D_{fibro}=D_{normal}/85$, the conduction delay time was closest to the experimental value (30 msec). Therefore we choose $D_{fibro}=D_{normal}/85$ as value of fibroblast conductivity in our tissue computation.

Along with the value of the fibroblast conductivity, we assumed that 5% additional fibroblasts were added to tissue. In the computation, the fibroblasts were distributed randomly over the entire anisotropic tissue domain with three cell kinds through thickness and their volume was set to 5% of the normal tissue volume. Fig. 8 represented the spiral wave formation in the hypertropic tissue with 5% additional fibroblasts. Unlike the normal case of anisotropic tissue, a secondary spiral wave was generated as shown in Fig. 8(d), (e), and (f), indicating that the pattern change from a single focus to a multi-focused reentrant wave could be made. This can eventually result in irregular reentrant wave inducing ventricular fibrillation.

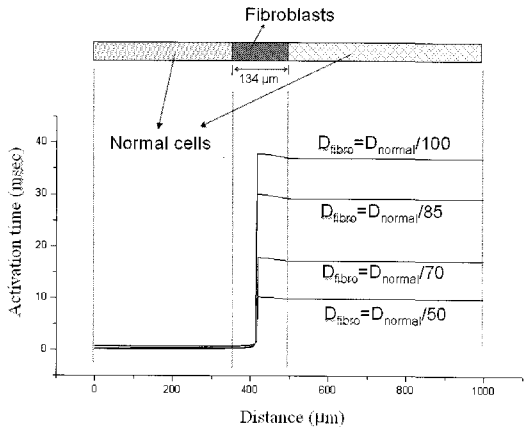

Figure 7. Activation delay time according to the values of fibroblast electric conductivity in the one dimensional model of the cardiac cell line with non-excitable fibrobalsts.

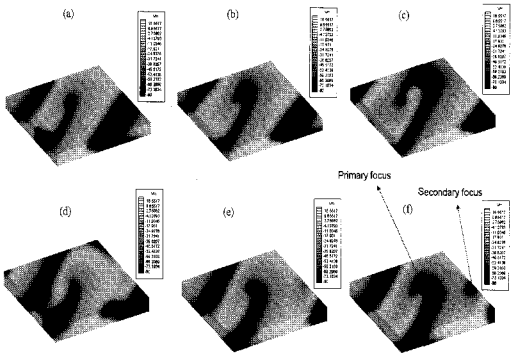

Figure 8. Sequential contours of the action potential in the hypertropic tissue model.

Discussions

In this study, we developed a mono-domain model to simulate three-dimensional reentrant wave propagation in a human cardiac tissue. The present model was based on the human cardiac cell model proposed by ten Tusscher *et al.* (TNNP model) (2004) and a mono-domain approximation for action potential propagation. The mono-domain method for electric wave propagation implemented by a finite element method was used to simulate the cardiac tissue propagation mechanism. Three types of cardiac cell models and anisotropic effect of fiber orientation was also incorporated in this model.

A typical shape of the membrane action potential using the TNNP model was well reproduced, showing a spike-notch-dome style pattern of human ventricular cell (Fig. 2). The three-dimensional simulation of isotropic cardiac tissue showed a single focused and regular spiral wave with no variation across thickness (Fig. 4). On the other hand, action potential gradient along fiber orientation and across thickness was observed in the anisotropic tissue model with three cell layers (Fig. 5). The pseudo ECG transient was oscillatory and had a reduced frequency, different from that of isotropic case (Fig. 6).

To test the reentrant wave under pathological state, we simulated a hypertopic model having additional non-excitable fibroblasts generated by a stochastic method (Fig. 7). Compared with normal tissue, the hypertropic tissue results showed a secondary focus of reentrant wave, indicating that the wave pattern can be more easily changed from regular with a concentric focus to irregular multi-focused reentrant waves that might cause arrhythmia or ventricular fibrillation (Fig. 8).

References

1. Berenfeld O, Jalife J. Purkinje-muscle reentry as a mechanism of polymorphic ventricular arrhythmias in a 3-dimensional model of the ventricles. Circ Res. 1998 Jun 1;82(10):1063-77.
2. Clayton RH, Holden AV. A method to quantify the dynamics and complexity of re-entry in computational models of ventricular fibrillation. Phys Med Biol. 2002 Jan 21;47(2):225-38.
3. Fenton FH, Cherry EM, Hastings HM, Evans SJ. Multiple mechanisms of spiral wave breakup in a model of cardiac electrical activity. Chaos. 2002 Sep;12(3):852-892.
4. Gaudesius G, Miragoli M, Thomas SP, Rohr S. Coupling of cardiac electrical activity over extended distances by fibroblasts of cardiac origin. Circ Res. 2003 Sep 5;93(5):421-8.
5. Gima K, Rudy Y. Ionic current basis of electrocardiographic waveforms: a model study. Circ Res. 2002 May 3;90(8):889-96.
6. Matsuoka, S., Sarai, N., Kuratomi, S., Ono, K., Noma, A. Role of individual ionic current systems in ventricular cells hypothesized by a model study. Jpn. J. Physiol. 2003 53, 105-23.
7. Noble D, Varghese A, Kohl P, Noble P. Improved guinea-pig ventricular cell model incorporating a diadic space, IKr and IKs, and length- and tension-dependent processes.

Can J Cardiol. 1998 Jan;14(1):123-34.

8. Priebe, L., Beuckelmann, D.J., Simulation study of cellular electric properties in heart failure. Circ. Res. 1998, 82, 1206–1223.
9. Qu Z, Garfinkel A. An advanced algorithm for solving partial differential equation in cardiac conduction. IEEE Trans Biomed Eng. 1999 Sep;46(9):1166-8.
10. Rudy Y. From genome to physiome: integrative models of cardiac excitation. Ann Biomed Eng. 2000 Aug;28(8):945-50.
11. Ten Tusscher, K.H.W.J., Noble, D., Noble, P.J., Panfilov, A.V., A model for human ventricular tissue. Am. J. Physiol. Heart Circ. Physiol. 2004, 286, H1573–H1589.
12. Usyk TP, McCulloch AD. Electromechanical model of cardiac resynchronization in the dilated failing heart with left bundle branch block. J Electrocardiol. 2003;36 Suppl:57-61.
13. Xie F, Qu Z, Yang J, Baher A, Weiss JN, Garfinkel A. A simulation study of the effects of cardiac anatomy in ventricular fibrillation. J Clin Invest. 2004 Mar;113(5):686-93.